Validation of anatomy-enhanced cardiac FDG-PET imaging: an ex vivo sheep study

A. Turco[1], J. Duchenne[2], J. Nuyts[1], O. Gheysens[1], J.U. Voigt[2], P. Claus[2], K. Vunckx[1]

I. Introduction

PET images suffer from partial volume effects (PVE) due to the poor spatial resolution of the PET system. Anatomy-enhanced PET reconstruction allows to restore such loss of resolution in PET images and attempt to reveal more accurately the actual tracer distribution [1] [4] .

The aim of this work is to assess the effectiveness of Maximum-A-Posteriori (MAP) reconstructions with the use of a CT-based anatomical prior for partial volume correction (PVC) of measured cardiac PET images. To rule out the effects of motion due to the beating heart and the respiration on the performance of the PVC technique, realistic static cardiac datasets obtained from a number of sacrificed sheep were used.

The obtained MAP reconstructions were compared to regular ordered-subsets expectation maximization (OSEM) with resolution recovery (RR) and to clinical reconstructions.

II. Methods

Section II-A describes the experimental workflow followed to obtain the datasets. The sections II-B and II-C describe the methods applied to reconstruct and analyse the ex vivo datasets. The techniques applied to an in vivo dataset are briefly described in the section II-D.

A. Experimental workflow

Three normal sheep and two sheep with induced dilated cardiomyopathy were injected with ^{18}F-FDG and scanned, 30 minutes post injection, on the Siemens Biograph 16 PET/CT (Hirez) for 30 minutes. A low dose, low pitch CT for attenuation correction (AC) was also acquired. Throughout the experiment, the sheep were actively ventilated to maintain a regular breathing. Triggers corresponding to the breathing and beating peaks were acquired with an Anzai respiratory gating system and an ECG machine, respectively, and stored in the PET listmode. The sheep had been previously scanned on a Siemens SOMATOM Definition Flash scanner. In order to obtain a high-resolution cardiac CT, the sheep was forced into a prolonged expiration by temporarily disconnecting the ventilator. This allowed us to determine the phase of the breathing during the scan.

After these scans, the sheep were sacrificed and had their heart excised. Each heart was immediately filled with a very low-attenuating, hardening foam, to ensure shape stability throughout all subsequent scans. Next, it was positioned in a Siemens Focus220 microPET scanner for a 15-minute PET scan, followed by a 10-minute transmission scan (using a ^{57}Co point source) for AC. The high spatial resolution (1.5 mm), almost PVE-free images generated with the microPET served as gold standard to which all other reconstructions were compared. The hearts were then transferred to the Hirez scanner and positioned in the same way as in the microPET.

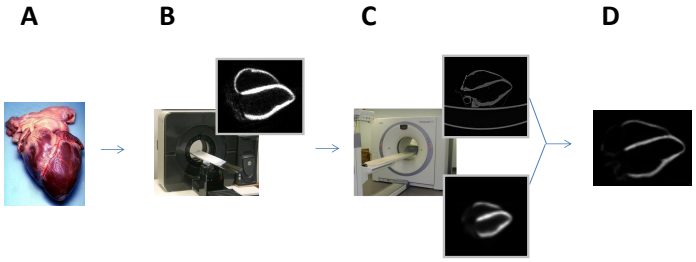

Fig. 1. Experimental workflow for the ex vivo scans. A) The sheep is sacrificed and the heart is excised. B) The heart undergoes a 15-minute microPET scan, followed by a 10-minute transmission scan on the same camera. C) The heart undergoes a 20-minute PET scan on the Hirez scanner, followed by a high-resolution CT scan (for AC and PVC). D) PVC is applied and the resulting reconstruction is compared to the microPET image (B).

A a 20-minute PET scan was then performed, followed by a high-dose, high resolution CT (HRCT). The CT served for both accurate AC and for PVC. Figure 1 summarizes the experimental workflow for the ex vivo part.

B. PET reconstructions

The microPET list-mode datasets were rebinned into sinograms and reconstructed using 3D OSEM (5 iterations x 28 subsets) modelling the resolution of the scanner. A spatially invariant Gaussian kernel with a FWHM of 1.3 mm, applied in image space, was used. For a more accurate correction for attenuation, the HRCT from the Hirez scanner was used as AC map for the microPET. To this end, the HRCT was first rigidly registered (using normalized cross correlation as similarity metric) to an initial microPET reconstruction corrected for AC with its corresponding transmission scan. The resulting HRCT was then converted to 511 keV attenuation values and used as AC map for a subsequent microPET reconstruction, using in-house developed software. 3D OSEM with a [3, 2, 2] x [42, 24, 1] (iterations x subsets) iteration scheme was also used to reconstruct all Hirez datasets. Reconstructions with and without resolution recovery (RR) were performed. When RR was applied, a stationary Gaussian point spread function of 4.35 mm/4.15 mm (transaxial and axial values, respectively) modelled in image space was used. In addition, MAP reconstructions with RR and CT-based anatomical information were performed and compared to the standard OSEM. All datasets were precorrected for scatter and randoms, and sensitivity and attenuation (using the HRCT) were modelled during reconstruction.

The anatomical information is included by means of the Bowsher prior [2], in its modified asymmetrical version [3]. Bowsher reconstructions with different prior weights, neighbourhood sizes and number of neighbours were performed. The HRCT was used as anatomical information.

A reconstruction performed by the Hirez, using a pre-set clinical reconstruction protocol (2D OSEM, 5 iterations and 8 subsets, without RR and post-smoothed with a Gaussian of FWHM = 2 mm), was also introduced in the comparison.

[1] KU Leuven - University of Leuven, Department of Imaging and Pathology, Nuclear Medicine and Molecular imaging, Medical Imaging Research Center (MIRC), B-3000 Leuven, Belgium. [2] KU Leuven - University of Leuven, Department of Cardiovascular Sciences, Cardiology, Medical Imaging Research Center (MIRC), B-3000 Leuven, Belgium.

This work is supported by KU Leuven grant OT/12/084 and the Research Foundation - Flanders (FWO)

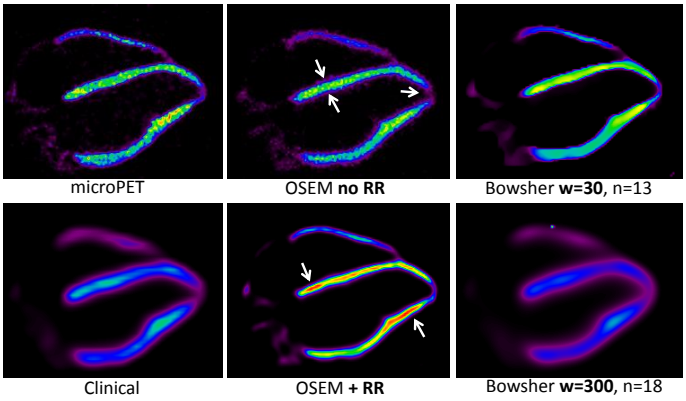

Fig. 2. Comparison of different Hirez reconstructions to the microPET image (ground truth). w : weight of the prior, n : number of selected neighbours of the prior

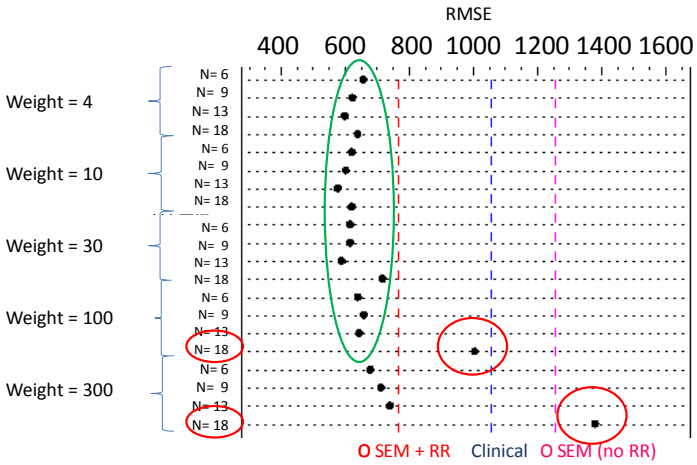

Fig. 3. Root Mean Square Errors for an ex vivo dataset. The use of different Bowsher parameters, particularly of the weight and the number of selected neighbours, plays a role in the similarity to the gold standard.

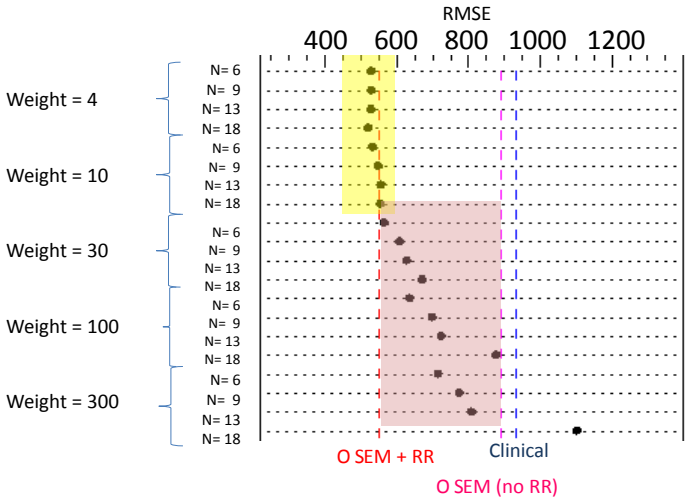

Fig. 4. Root Mean Square Errors for another ex vivo sheep dataset. The results of the anatomy-enhanced reconstructions do not show the same, obvious improvements as in Fig. 4.

C. Comparison and evaluation of the reconstructions

All reconstructions were compared to the gold standard provided by the microPET image, which was rigidly registered to the Hirez 3D OSEM+RR reconstruction using the sum of squared differences as similarity metric. Visual inspection of the resulting images was followed by the calculation of the root mean square error (RMSE) between the microPET image and the reconstructed images. In order to take into account only the contribution of the myocardium during the calculation of the RMSE, a mask image was computed by thresholding the corresponding HRCT to the cardiac muscle and subsequently dilating the resulting mask with a [7, 7, 7] kernel. All reconstructions were multiplied by such mask before the calculation of the RMSE. Small discrepancies with regards to total reconstructed activity were still present between the microPET images and our reconstructions. For this reason, all images were first normalized to the total activity of the microPET and only then the RMSE was calculated. More specifically, each Hirez reconstruction was divided by the total activity of the 3D OSEM + RR and then multiplied by the total activity of the masked microPET.

D. Application to in vivo datasets: a proof of principle

A first attempt to apply PVC on in vivo datasets was also performed. Phase-based gating for respiration using in-house developed software was performed on the full 30-minute listmode PET. The respiratory gate corresponding to the expiration phase was further divided into 10 cardiac gates, all rebinned into sinograms and reconstructed using AC-OSEM. The HRCT acquired in the Flash scanner was then registered to each of the reconstructed cardiac gates using normalized mutual information as similarity metric. Upon visual inspection it was found which PET gate corresponded most accurately to the cardiac phase in which the HRCT was acquired.
Only the cardiac sinogram of that PET gate was therefore reconstructed, using the Hirez CT of the same cardiac gate for AC and the registered HRCT for anatomical information. In addition to a regular 3D OSEM with resolution recovery, the asymmetrical Bowsher was used for PVC reconstruction.

III. Results

Fig. 2 shows the different activity distributions for an ex vivo dataset (normal sheep) obtained when different reconstruction strategies were used, in comparison to the ground truth represented by the microPET image. It is interesting to notice how the estimated activity distribution changes when only the prior parameters are modified (e.g. weight, number of Bowsher neighbors of interest. Cfr top-right and bottom-right images of Fig. 2).

Fig. 3 shows the influence of the different parameters on the RMSE for another of the analysed datasets (normal sheep). A clear difference in RMSEs can be noted between reconstructions with and without RR, with further improvements when anatomical information is included. Furthermore, it is confirmed that a bad selection of the parameters for the Bowsher (namely, a too high prior weight and an excessive number of neighbors) can worsen the similarity between the Hirez reconstruction and the gold standard.

The results presented in Fig. 3 describe the best-case scenario, where the predictions of superiority of the anatomy-enhanced reconstructions is confirmed. For some other datasets, the same graph shows less obvious improvements (see Fig. 4) and a worsening of the similarity metric as soon as the weight of the prior is increased. We are currently investigating possible reasons for such discrepancy.

Fig. 5 shows the result obtained after application of the PVC method to the in vivo dataset of a normal sheep, after double-gating of the initial listmode file. The first results are encouraging, showing better edge delineation and a more homogeneous distribution of activity, as expected in a heart in normal physiological conditions.

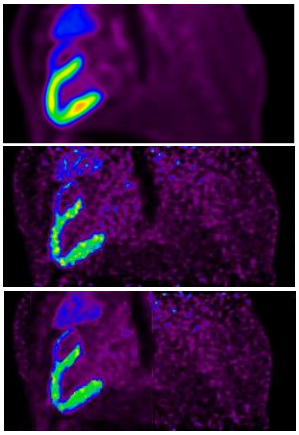

Fig. 5. First results of the application of the asymmetrical Bowsher prior to a double-gated in vivo dataset. The non-gated clinical standard (top) is compared to an OSEM reconstruction with RR (middle) and to a Bowsher reconstruction (bottom).

IV. Discussion and conclusions

The modelling of the spatial resolution of the scanner resulted into sharper images and restored activity within the myocardial walls. The additional use of anatomical information reduced the Gibbs artefacts induced by the RR, resulting in visual improvements in volume delineation and uniformity of activity values. The Bowsher prior required fine tuning of the parameters in order to obtain such improvements. It has to be noted that so far not all datasets led to the same conclusions. We are currently analysing possible reasons for this different behaviour.

Future work includes a more accurate analysis of the results obtained so far, in order to detect possible flaws or inaccuracies in the experimental setup or in the data processing. After full validation of anatomy-enhanced reconstructions on ex vivo datasets, the in vivo analysis will be extended and the results will be compared to the corresponding ex vivo microPET images.

V. Acknowledgements

The authors wish to thank C. Watson, J. Jones et al. for their help in the Siemens data processing.

References

[1] Alessio, A.M. and Kinahan, P.M. “Improved quantitation for PET/CT image reconstruction with system modeling and anatomical priors.” *Med. Phys* 2006;33:4095-4103

[2] Bowsher J.E., Hong Yuan, Hedlund L.W., Turkington T.G., Akabani G., Badea A., Kurylo W.C., Wheeler C.T., Cofer G.P., Dewhirst M.W.and Johnson G.A., “Utilizing MRI information to estimate F18-FDG distributions in rat flank tumors”, *IEEE Nucl. Sci. Symp. Conf. Rec.*, pp.2488 -2492 2004

[3] Vunckx K., Nuyts J., “Heuristic Modification of an Anatomical Markov Prior Improves its Performance”, *IEEE Nucl. Sci. Symp. Conf. Rec.*, 3:3262-3266 2010

[4] Vunckx K., Atre A., Baete K., Reilhac A., Deroose C.M., Van Laere K, Nuyts J.,“Evaluation of three MRI-based anatomical priors for quantitative PET brain imaging.”, *IEEE Trans. Med. Imaging* 2012, 31(3):599612